Cancer Research

Angiocrine Factors Modulate Tumor Proliferation and Motility through EphA2 Repression of Slit2 Tumor Suppressor Function in Endothelium

Dana M. Brantley-Sieders, Charlene M. Dunaway, Meghana Rao, et al.

Cancer Res 2011;71:976-987. Published OnlineFirst December 8, 2010.

Published OnlineFirst December 8, 2010; DOI:10.1158/0008-5472.CAN-10-3396

Cancer Research

Angiocrine Factors Modulate Tumor Proliferation and Motility through EphA2 Repression of Slit2 Tumor Suppressor Function in Endothelium

Dana M. Brantley-Sieders[1], Charlene M. Dunaway[1], Meghana Rao[2], Sarah Short[2], Yoonha Hwang[1], Yandong Gao[3], Deyu Li[3], Aixiang Jiang[2,4], Yu Shyr[2,4], Jane Y. Wu[5], and Jin Chen[1,2,6,7]

Abstract

It is well known that tumor-derived proangiogenic factors induce neovascularization to facilitate tumor growth and malignant progression. However, the concept of "angiocrine" signaling, in which signals produced by endothelial cells elicit tumor cell responses distinct from vessel function, has been proposed, yet remains underinvestigated. Here, we report that angiocrine factors secreted from endothelium regulate tumor growth and motility. We found that Slit2, which is negatively regulated by endothelial EphA2 receptor, is one such tumor suppressive angiocrine factor. Slit2 activity is elevated in EphA2-deficient endothelium. Blocking Slit activity restored angiocrine-induced tumor growth/motility, whereas elevated Slit2 impaired growth/motility. To translate our findings to human cancer, we analyzed EphA2 and Slit2 expression in human cancer. EphA2 expression inversely correlated with Slit2 in the vasculature of invasive human ductal carcinoma samples. Moreover, analysis of large breast tumor data sets revealed that Slit2 correlated positively with overall and recurrence-free survival, providing clinical validation for the tumor suppressor function for Slit2 in human breast cancer. Together, these data support a novel, clinically relevant mechanism through which EphA2 represses Slit2 expression in endothelium to facilitate angiocrine-mediated tumor growth and motility by blocking a tumor suppressive signal. *Cancer Res; 71(3); 976–87. ©2010 AACR.*

Introduction

Angiogenesis, the process of generating new blood vessels sprouts from existing vasculature, promotes tumor progression through delivery of oxygen and nutrients and providing a point of entry into circulation that enables metastatic cells to metastasize (reviewed in ref. 1). High expression levels of proangiogenic factors and/or elevated microvascular density have been correlated with malignant progression and a poor prognosis in patients suffering from several types of cancer, including breast cancer (reviewed in refs. 2–5). Investigation into the molecular mechanisms that regulate tumor angiogenesis identified many host and tumor-derived angiogenic and angiostatic factors, whose misregulation contributes to tumor neovascularization (reviewed in refs. 5–7). Although endothelial cell responses to tumor signals have been investigated, molecular signals released by endothelial cells that may affect tumor cell behavior have yet to be identified. Butler and colleagues (8) recently proposed that endothelial cells produce "angiocrine" factors that could enable tumor growth, motility, and ultimately metastasis. In addition to production of factors that stimulate tumor cell growth and invasion, tumor endothelium may also downregulate tumor suppressive factors as a component of angiocrine-mediated signaling.

EphA2 receptor tyrosine kinase was recently shown to regulate tumor angiogenesis, and is often overexpressed in tumor vasculature (reviewed in refs. 9–11). However, the potential role of EphA2 receptor in angiocrine signaling has not yet been investigated. We report here that breast cancer growth and motility were enhanced by angiocrine factors produced by wild-type endothelium relative to EphA2-null endothelium. Microarray and protein expression/function analyses revealed that EphA2 deficiency enhances expression of Slit2. *Drosophila* Slit and its vertebrate homologs, Slits 1–3, function as repulsive cues that restrict improper patterning of commissural axons through interaction with the roundabout (Robo) family of receptors (reviewed in ref. 12). The role of Slit2 in tumor progression versus suppression, however, remains controversial, with studies supporting both inhibition of tumor growth/metastasis or promotion of these processes

Authors' Affiliations: [1]Departments of Medicine and [2]Cancer Biology, Vanderbilt University School of Medicine, Nashville, Tennessee; [3]Department of Mechanical Engineering, Vanderbilt University, Nashville, Tennessee; [4]Department of Biostatistics, Vanderbilt University School of Medicine, Nashville, Tennessee; [5]Department of Neurology and Center for Genetic Medicine, Northwestern University Feinberg School of Medicine, Robert H. Lurie Comprehensive Cancer Center, Chicago, Illinois; [6]Veterans Affairs Medical Center, Tennessee Valley Healthcare System, Nashville, Tennessee; and [7]Department of Cell and Developmental Biology, Vanderbilt University School of Medicine, Nashville, Tennessee

Note: Supplementary data for this article are available at Cancer Research Online (http://cancerres.aacrjournals.org/).

Corresponding Author: Jin Chen, Vanderbilt University School of Medicine, A-4323 MCN, 1161 21st Avenue South, Nashville, TN 37232-2363. Phone: 615-343-3819; Fax: 615-343-8648. Email: jin.chen@vanderbilt.edu

doi: 10.1158/0008-5472.CAN-10-3396

Published OnlineFirst December 8, 2010; DOI:10.1158/0008-5472.CAN-10-3396

in breast and other cancers (13–19). We found that blocking Slit activity in EphA2-deficient endothelium restored angiocrine-induced tumor growth/motility. Conversely, elevated Slit2 impaired growth/motility induced by wild-type endothelium. EphA2 expression inversely correlated with Slit2 in the vasculature of invasive human ductal carcinoma samples, and analysis of large breast tumor data sets revealed that Slit2 correlated positively with overall and recurrence-free survival, providing clinical validation for the tumor suppressor function for Slit2 in human breast cancer. Together, these data support a new, clinically relevant mechanism through which EphA2 receptor tyrosine kinase represses Slit2 tumor suppressor in endothelium to promote angiocrine-mediated tumor growth and migration in breast cancer.

Materials and Methods

Reagents

Antibodies against the following proteins were used: EphA2 (Zymed Laboratories; Santa Cruz Biotechnology; Millipore); actin, phosphotyrosine PY99 and PY20, Robo1, Robo4, and normal rabbit immunoglobulin G (IgG; Santa Cruz Biotechnology); E-cadherin and myc (BD Biosciences); Slit2 (Sigma-Aldrich); CD31 (Angio-Proteomie); von Willebrand factor (vWF; Zymed Laboratories); proliferating cell nuclear antigen (PCNA; LabVision Corporation/Thermo Fisher Scientific). Recombinant rat Robo1-Fc, human IgG, and recombinant Slit2 were purchased from R&D Systems. Growth factor–reduced Matrigel was purchased from BD Biosciences. TO-PRO-3 iodide and 4′,6-diamidino-2 phenylindole dihydrochloride (DAPI) nuclear stains were purchased from Invitrogen, and Sigma-Aldrich, respectively. 5-Bromo-2-deoxyuridine (BrdU) was purchased from Sigma-Aldrich, and BrdU detection kit from Invitrogen.

Cell culture

Primary murine pulmonary microvascular endothelial cells were isolated from wild-type or EphA2-deficient animals as described previously (20). Cells were maintained in EGM-2 medium supplemented with penicillin-streptomycin and 10% fetal bovine serum. Wild-type or EphA2-deficient lung microvascular endothelial cells were isolated from 1- to 3–month-old mice derived from the H-2Kb-tsA58 transgenic "Immortomouse" background (21) as described previously (22) and grown at 33°C in EGM-2 medium supplemented with interferon-γ (10 ng/mL; Millipore) to permit stable expression of the temperature sensitive SV40 T-antigen (TAg) transgene. Prior to experimental manipulation, cells were incubated at 37°C for at least 3 days in the absence of interferon to downregulate TAg expression and revert the cells to a non-immortalized state.

4T1 mouse mammary adenocarcinoma cells were obtained from ATCC. The NeuTC cell line derived from MMTV-Neu mammary epithelial tumors were generously provided by Dr. Carlos Arteaga and maintained as described previously (23). MDA-MB-231 and MCF7 human breast adenocarcinoma cells were purchased from American Type Culture Collection (ATCC). Cells were maintained in Dulbecco's modified Eagle's medium (DMEM) supplemented with penicillin-streptomycin and 10% fetal bovine serum. To generate conditioned medium (CM) from tumor cells and endothelial cells, 1×10^6 cells were plated in 10-cm dishes and grown to approximately 75% confluence in normal growth medium, then incubated in 3 mL of Opti-MEM medium supplemented with 2% fetal calf serum (FCS) for 48 hours. CM was collected and filtered prior to use. For some studies, CM was concentrated using Amicon Ultra centrifugal filtration devices (Millipore).

Microarray and real-time qRT-PCR analyses

We assessed differential gene expression in Immorto wild-type versus EphA2-deficient lung microvascular endothelial cells that were cultured CM generated from 4T1 tumor cells. Total RNA from duplicate sets of endothelial cells was isolated using Trizol (Invitrogen) as per the manufacturer's protocol, then amplified and hybridized to Affimetrix Mouse Gene 1.0 arrays by the Vanderbilt University Microarray Shared Resource Core Facility. Out of approximately 35,400 genes analyzed, 99 candidates displayed differences in expression between wild-type versus EphA2-deficient cells of greater than 2-fold. One of the soluble factor candidates selected for analysis was Slit2.

Expression of *slit2* mRNA in endothelial cells was validated by quantitative RT-PCR (qRT-PCR) analysis, using the following primers: Slit2 Fwd (20mer) 5′-agg gaa gat gag tgg cat tg-3′ (240>259; NM_178804.2), Slit2 Rev (20mer) 5′-gtg cct gag acc agc aaa at-3′ (486>467; NM_178804.2); and control 18S ribosomal RNA primers: Fwd (20mer) 5′-caa ctt tcg atg gta gtc gc-3′, Rev (21mer) 5′-cgc tat tgg agc tgg aat tac-3′. Real-time PCR was performed using a StepOnePlus Real-Time PCR System from Applied Biosciences with iQ SYBR supermix from BioRad. We used a 2-step amplification (40 cycles of 95°C, 15 seconds; 60°C, 30 seconds; followed by melting temperature determination stage) and quantified relative changes in gene expression using the DDCt method as per manufacturer's instructions.

Recombinant Slit2 production

The HEK293 cells that produce full-length Slit2 proteins tagged with c-myc have been described (24). The cells were cultured in DMEM with 5% FCS. Slit2 was partially purified from the supernatants as described previously (24). The supernatant from parental HEK cells was used as controls. Working concentrations of Slit2 from diluted supernatants was estimated to be between 100 and 250 ng/mL on the basis of silver staining of serial dilutions of supernatants following SDS-PAGE fractionation, and comparable concentrations of commercially prepared Slit2 from R&D Systems were also used. The 100–250 ng/mL doses used were selected on the basis of similar effective dose ranges published studies (25–27).

In vitro proliferation, apoptosis, and migration assays

We established 3-dimensional (3D) spheroid cultures as described previously (28, 29). Cultures were maintained in endothelial CM or 2% FCS base medium for 5 days prior to photodocumentation. Digital images were scored for spheroid

Published OnlineFirst December 8, 2010; DOI:10.1158/0008-5472.CAN-10-3396

culture area in 4 random fields in 3 cultures per field using NIH ImageJ software. For confocal imaging, spheroid cultures were fixed in 10% neutral buffered formalin and subjected to immunostaining for E-cadherin followed by nuclear staining with TO-PRO-3 as previously described (29). Tumor cell growth and survival in culture was assessed in response to treatment with endothelial cell CM versus 2% FCS base medium using methods described previously (29) by BrdU incorporation (BrdU staining kit; Invitrogen) and terminal deoxynucleotidyl transferase–mediated dUTP nick end labeling (TUNEL; Apoptag Red *in situ* apoptosis detection kit, Millipore), respectively. Tumor cell migration was assessed in response to endothelial cell CM versus 2% base medium as described in our previous studies (29) by transwell assays. For Slit activity modulation studies, endothelial CM was supplemented with control IgG or Robo1-Fc (0.1 μg/mL), Slit2 (100 ng/mL recombinant or HEK293 supernatant), or control HEK293 supernatant. The percentage of BrdU or TUNEL+ nuclei relative to total nuclei was quantified in 4 random 20× fields in duplicate samples for each experiment in 3 independent experiments/condition.

Tumor-endothelial cell cross-migration was assessed using microfluidic platforms fabricated by bonding polydimethylsiloxane (PDMS; Ellsworth Adhesives) layers to glass microscope coverslips. The first PDMS layer is comprised of 2 cell culture chambers ($6 \times 0.7 \times 0.06$ mm) separated by a 100-μm wide PDMS valve barrier, with each chamber connected to a nutrient reservoir and a waste well through microchannels. This layer is bound to a glass coverslip (VWR Vista Vision) and the cell culture chamber is aligned to a region where the glass coverslip is etched to 8- to 10-μm deep using buffered hydrofluoric acid. The second PDMS layer, defining a control chamber ($16 \times 5 \times 1$ mm), is aligned and bonded on top of the first PDMS layer. Before bonding, all surfaces except those of the valve barrier and the etched region on the coverslip were treated with oxygen plasma. Therefore, other than the contact between the valve barrier and the coverslip, the PDMS and the coverslip formed strong irreversible bonding. Depending on the pressure in the control chamber, the valve barrier could be either pushed down or released in an "up" position. In the "up" position, the gap between the bottom of the PDMS valve barrier and the surface of the etched coverslip allowed for interaction and communication between the 2 cell populations (Fig. 1D). In the down position, the valve barrier completely isolates the 2 chambers for separate culture or treatment of each cell population.

Cell chambers were coated with growth factor–reduced Matrigel and the PDMS barrier was pushed down by pressurizing the control chamber with deionized water. 4T1-GFP labeled tumor cells (1×10^6) were loaded into one side of the chamber and Cell-Tracker Orange (Molecular Probes; ref. 30) labeled endothelial cells (1×10^6) were loaded into the other side. After 24 hours, we replaced growth medium with starvation medium (Optimem/2% FCS) and released the barrier to permit cross-migration, which was scored 24 hours later by counting tumor cells (green) and endothelial cells (red) that crossed the central valve barrier in 4 independent 10× field views per device.

In Vivo tumor cell–endothelial cell cotransplantation studies

All animals were housed under pathogen-free conditions, and experiments were performed in accordance with AAALAC (Association for assessment and accreditation of laboratory animal care) guidelines and with Vanderbilt University Institutional Animal Care and Use Committee approval. Tumor cell–endothelial cell cotransplantation experiments were performed as described previously (22, 30). Briefly, wild-type or EphA2-deficient endothelial cells were transduced with 1×10^8 plaque-forming units/mL of β-galactosidase (β-gal) adenovirus. 4T1 tumor cells (5×10^4 cells) and Ad-β-gal–transduced endothelial cells (5×10^5) were resuspended in 300 μL of growth factor–reduced Matrigel and injected into the subcutaneous dorsal flank of 10–week-old nude female mice (Harlan-Sprague-Dawley). Tumors were collected 2, 4, and 7 days posttransplantation and tumor volume was assessed using the following formula: volume = length × width^2 × 0.52. Cryosections were processed first for X-gal staining and then subjected to immunohistochemistry for PCNA or TUNEL as described previously (30). PCNA or TUNEL+ nuclei were quantified the periphery of the tumor plug, as defined by a depth of no more than 100 μm from the margin to the plug interior and greater than 200 μm distance from any LacZ+ exogenous endothelial cell. PCNA and TUNEL+ nuclei were also quantified in the interior of the plug for tumor cells adjacent to LacZ+ exogenous endothelial cells, within 5 to 50 μm. Data are a representation of 8 independent tumors/condition from 2 independent experiments.

Tumor-endothelial CM cotransplantation assays were performed as described earlier in the text, using CM from wild-type or EphA2-deficient cultured endothelial cells, versus base medium (Optimem/2% FCS) or Optimem control medium. 4T1 tumor cells (1×10^5) were resuspended in 50 μL of 20× concentrated CM or Optimem (final concentration 5×) plus 150 μL growth factor–reduced Matrigel ± 0.5 mg recombinant Slit2, 2.5 mg recombinant Robo1-Fc, or 2.5 mg control IgG. The mixture was injected subcutaneous into recipient nude female mice and growth of resulting tumors scored as described earlier in the text. On day 7, mice were injected intraperitoneally with 10 mg/mL BrdU/PBS (100 μL/10 gm body weight) and tumor harvested 2 hours after injection for analysis.

Immunoblot and immunoprecipitation analyses

Prior to stimulation and lysis for immunoprecipitation/immunoblot, tumor cells were serum starved for 24 hours in Opti-MEM + 2% FCS. Robo1 was immunoprecipitated from approximately 500 μg of tumor cell lysate prepared in RIPA buffer plus protease and phosphatase inhibitors using anti-Robo1 antibodies (0.5 μg each Santa Cruz H-200 and I-20 clones) plus protein A/G-sepharose beads (50 μL, Santa Cruz Biotechnology). EphA2 was immunoprecipitated from 500 μg endothelial cell lysate as described previously (20, 31). For validation of Slit activity in endothelial cell CM, tumor cells were stimulated with 5× concentrated CM from wild-type versus EphA2-deficient endothelial cells versus 2% FCS base medium as a negative control, and partially purified myc-Slit2 from HEK293 producer cells or parental, negative control cells,

Published OnlineFirst December 8, 2010; DOI:10.1158/0008-5472.CAN-10-3396

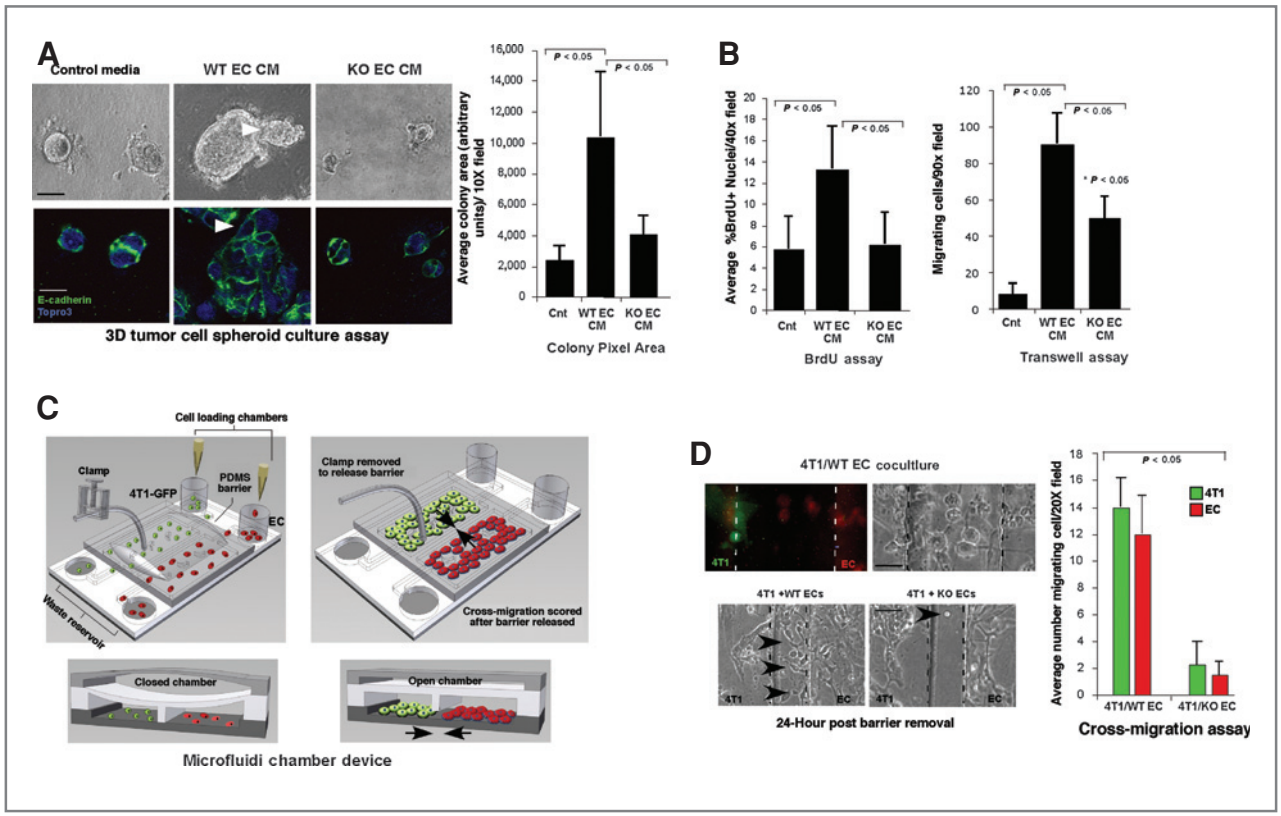

Figure 1. "Angiocrine" signals from endothelial cells enhance tumor cell growth and motility, which is diminished in the absence of endothelial EphA2 receptor function. A, top, photomicrographs of 4T1 tumor cell spheroids cultured in control base medium (Optimem/2% FCS) versus CM from WT or KO EC. Bottom, confocal images of spheroids stained with E-cadherin (green) and Topro3 (blue) nuclear counterstain. Arrowheads indicate invasive protrusions. Colony size was quantified on the basis of pixel area of 4 independent colonies/photomicrograph in replicate cultures from 3 to 5 independent experiments. Scale bar = 25 μm (top), 10 μm (bottom). B, 4T1 tumor cell proliferation in 2D culture was scored by BrdU incorporation, and 4T1 tumor cell migration was measured by transwell assay. C, schematic for microfluidic chamber device. Tumor cells (4T1-GFP, green) and endothelial cells (CellTracker Orange dye labeled, red) were seeded into 2 adjacent cell culture chambers separated by a narrow PDMS barrier. Release of the valve barrier permits cross-migration of both cell types through the central chamber. Arrows indicate direction of cross-migration through the open chamber on barrier removal. D, cross-migration of tumor cells and endothelial cells was quantified simultaneously on the basis of cell morphology and differential fluorescent labeling. Arrowheads indicate cells that migrated into the central chamber (boundaries between cell chambers and central chamber marked with dashed lines). Scale bar = 10 μm (top), 50 μm (bottom). Data are a representation of 3 to 5 independent experiments using CM/cells from at least 3 independent WT versus KO EC isolates for all cell culture experiments. Graphs display average ± SD.

for 15 minutes at 37°C. Lysate and/or immunoprecipitation products were fractionated on 10% to 12% SDS-polyacrylamide gels. The proteins were then transferred to nitrocellulose membranes and probed with primary antisera. Specific immunoreaction was detected using anti-IgG antibodies conjugated to horseradish peroxidase (Promega) and Pierce ECL chemiluminescence detection kit (Thermo Scientific). The blots were stripped and reprobed with anti-actin (Santa Cruz Biotechnology) antibodies to confirm uniform loading. Data are a representation of 3 to 5 independent experiments.

Histology and expression analyses

For immunofluorescence staining, EC were seeded onto Matrigel-coated 2-well Lab-Tek chamber slides (Nalgene-Nunc/Thermofisher Scientific) and grown for 24 hours. Cells were fixed for 2.5 minutes with 10% neutral buffered formalin (Fisher Scientific), washed, and stained for Slit2 and CD31 as per antibody manufacturer's instructions. Staining was detected using an Alexa-488–conjugated secondary antibody (Molecular Probes) followed by nuclear counterstain with DAPI. For tumor cell–endothelial cell cotransplantation studies, tumors were harvested, fixed for 5 minutes in 4% paraformaldehyde, and cryoembedded. Sections were stained with X-gal followed by immunohistochemistry for PCNA or TUNEL as described previously (30). For tumor cell–endothelial cell CM coinjection studies, tumors were harvested, fixed overnight in 10% neutral buffered formalin, and processed for paraffin-embedding. Staining/quantification for PCNA, TUNEL, and vWF was performed as described previously (29, 30, 32).

Analysis of *slit2* in the human breast cancer data sets (33–35) was performed in collaboration with the Vanderbilt-Ingram Cancer Center's Biostatistics Core Resource. Expression levels were analyzed in relation to overall and/or recurrence-free survival. Tissue microarrays (TMA) were purchased from Cybrdi, Inc. and stained for EphA2 as described previously (29, 30) and for Slit2 as per antibody manufacturer's

Published OnlineFirst December 8, 2010; DOI:10.1158/0008-5472.CAN-10-3396

instructions (Sigma-Aldrich rabbit anti-SLIT2 antibody HPA023088), validated by the Human Protein Atlas (http://www.proteinatlas.org).

Results

Angiocrine signals control tumor cell proliferation and survival and are regulated by EphA2 receptor tyrosine kinase

To determine whether angiocrine factors influence tumor cell behavior and whether EphA2 regulates angiocrine function, we compared 4T1 mammary tumor cell growth, survival, and migration in response to conditioned medium (CM) derived from wild-type (WT) or EphA2-deficient (KO) microvascular endothelial cells (EC). Relative to control base medium, tumor cells grown in WT EC CM formed significantly larger, more irregular spheroid colonies in 3D culture (Fig. 1A; ref. 28). By contrast, KO EC CM produced smaller, more uniform colonies. We observed similar effects in mouse NeuTC and MCF7 human breast cancer cell cultures (Supplementary Fig. S1). WT EC CM significantly increased proliferation and motility relative to control media or KO EC CM (Fig. 1B; Supplementary Fig. S2A and B), but did not affect apoptosis (data not shown). In addition, coculture between 4T1 and WT EC promoted cross-migration of both cell types in microfluidic chamber devices (Fig. 1D), which enabled us to quantify migration of the 2 cell populations simultaneously (schematic, Fig. 1C). By contrast, coculture with KO EC abrogated cross-migration (Fig. 1D). These data show that EC produce angiocrine signals that modulate tumor cell growth and motility in the absence of blood flow, and that these signals are regulated in part by EphA2 receptor tyrosine kinase.

To test these effects *in vivo*, we performed tumor cell–endothelial cell cotransplantation assays (schematic, Fig. 2A). Though we previously showed that exogenous WT EC incorporate into newly forming tumor vasculature within 7 days and enhance tumor volume (refs. 22, 30; Fig. 2C), these studies did not allow us to determine the effect of angiocrine signaling by EC adjacent to tumor cells prior to infiltration of tumor vessels. Thus, we scored proliferation of internal tumor cells, which were within 5 to 50 μm of exogenous EC and removed from host blood vessels, at earlier time points. Proliferation was significantly higher in tumor cells adjacent to WT EC versus KO EC at day 4 (Fig. 2B). We detected no change in proliferation of peripheral tumor cells in proximity to infiltrating host vessels (Fig. 2B). This correlated with a lower overall cell density in the tumor interior for KO EC transplants versus WT EC controls (Fig. 2B, right). Differences in tumor volume between WT versus KO EC cotransplants were apparent by day 4 and significant by day 7 (Fig. 2C), consistent with proliferation data. We observed a comparable increase in tumor growth *in vivo*, but no change in apoptosis or microvascular density, on coinjection of tumor cells with WT EC CM, versus KO EC CM or control medium (Fig. 2D; Supplementary Fig. S3), validating that effects conferred by EC were specific for soluble, angiocrine signals. These data suggest that angiocrine signals produced by WT EC confer a growth advantage to adjacent tumor cells *in vivo*, which is diminished in the absence of EphA2.

EphA2 negatively regulates Slit2 expression and Slit activity in endothelium

To identify angiocrine signal(s) regulated by EphA2, we performed microarray analysis comparing gene expression in WT versus KO EC. One of the candidate genes we identified was *slit2*. Real-time qRT-PCR analysis revealed an average 2.5-fold increase in *slit2* expression in KO versus WT EC (Fig. 3A), which was accompanied by elevated Slit2 protein expression in KO EC (Fig. 3B). KO EC displayed elevated basal phosphorylation of Robo4, an endothelial specific receptor that binds to Slit2 (Fig. 3C; reviewed in ref. 36). Moreover, KO EC CM stimulation enhanced Robo1 receptor phosphorylation in 4T1 tumor cells, similar to the effect of exogenous Slit2 (Fig. 3D), which was abrogated by soluble Robo1-Fc receptor pretreatment (Fig. 3D). Exogenous Slit2 was either prepared from HEK293 cells as described previously (24) and expression confirmed by immunoblot (Fig. 3D) or purchased from a commercial source. Together, these data show that *slit2* gene expression and Slit activity are elevated in EphA2-deficient endothelium, and suggest that EphA2 negatively regulates *slit2* expression in endothelium.

Modulating Slit activity affects angiocrine-mediated tumor growth and motility in the context of EphA2

On the basis of expression data, we hypothesized that elevated Slit2 in KO EC could contribute to reduced tumor proliferation and motility. WT EC CM supplemented with exogenous Slit2 produced significantly smaller, more regular tumor spheroids relative to control IgG (Fig. 4A). In contrast, KO EC CM supplemented with soluble Robo1-Fc, which inhibits Slit activity in EC CM, produced significantly larger colonies with a more irregular, invasive morphology relative to controls (Fig. 4A). Slit2 inhibited WT EC CM–induced tumor cell proliferation and migration, whereas Robo1-Fc partially restored tumor cell proliferation and motility induced by KO EC CM (Fig. 4B; Supplementary Fig. S2). These findings were confirmed in human MDA-MB-231 breast cancer cells (Supplementary Fig. S2), showing that these effects are relevant to human cancer. In addition, Slit2 significantly impaired cross-migration of tumor cells and WT EC in microfluidic chamber assays, whereas Robo1-Fc partially restored cross migration in tumor cell–KO EC cocultures (Fig. 4C). These data suggest that Slit2 impairs tumor cell growth and motility in response to EC, and that inhibiting Slit activity partially alleviates these effects in EphA2-deficient endothelial cells in which *slit2* levels are elevated.

Next, we tested the effect of modulating Slit activity on angiocrine-mediated tumor growth *in vivo*. WT EC CM supplemented with Slit2 produced smaller tumors 3 to 7 days postinjection relative to IgG control (Fig. 4D), with comparable volumes to those induced by KO EC CM. By contrast, inhibiting Slit activity in KO EC CM with Robo1-Fc restored tumor volumes to levels comparable to those induced by WT EC CM. Consistent with these data, Slit2 reduced WT EC CM–induced tumor cell proliferation *in vivo*, whereas Robo1-Fc enhanced tumor cell proliferation on coinjection with KO EC CM (Supplementary Fig. S3). These data suggest that angiocrine signals regulated by EphA2, including Slit2, modulate tumor growth *in vivo*.

Published OnlineFirst December 8, 2010; DOI:10.1158/0008-5472.CAN-10-3396

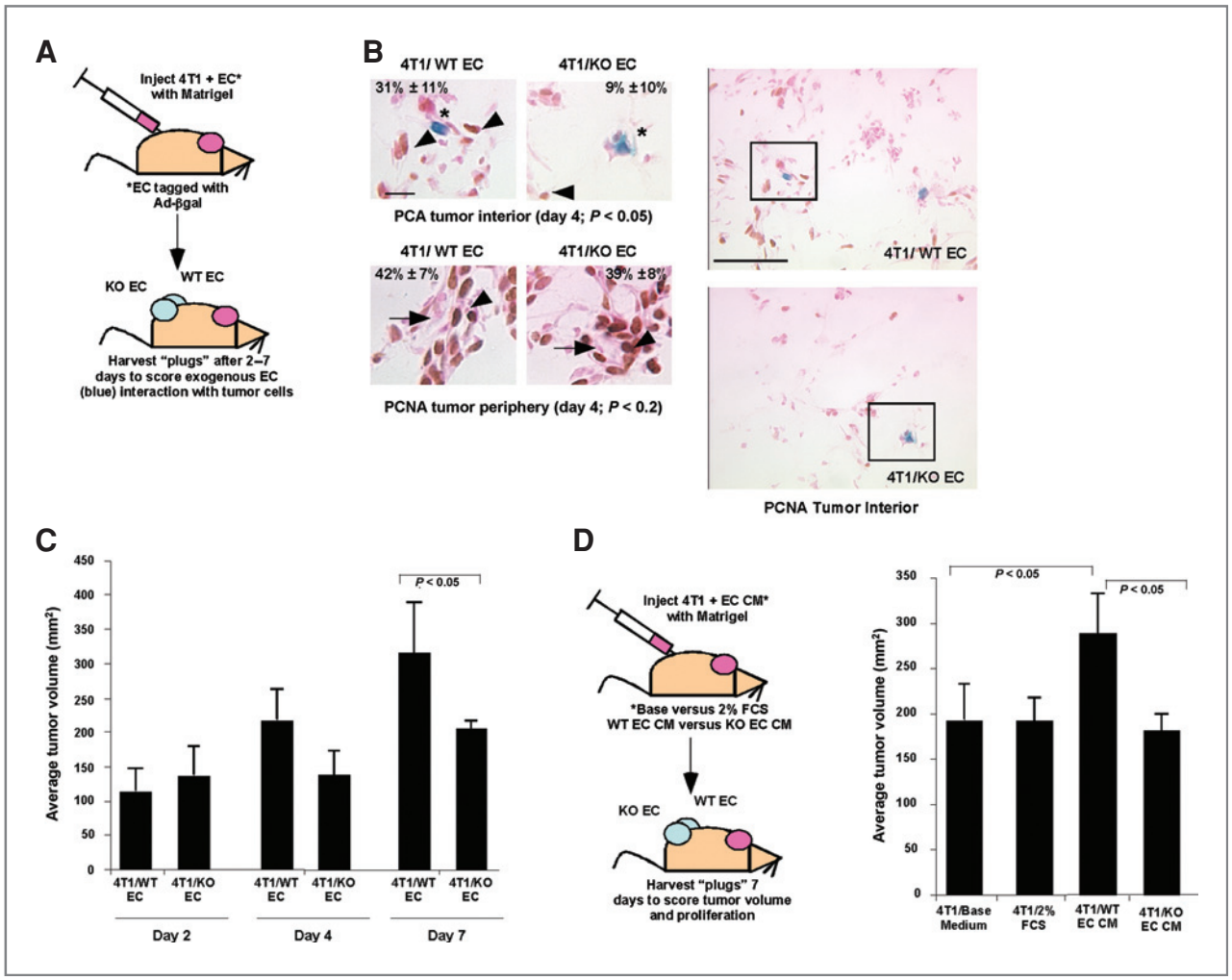

Figure 2. Effect of "angiocrine" signals from endothelial cells on tumor growth *in vivo*. A, schematic for tumor cell–endothelial cell cotransplantation experimental design. 4T1 tumor cells were ad-mixed with WT or KO EC (labeled with adenovirus encoding β-gal), resuspended in growth factor–reduced Matrigel, and injected subcutaneously into the dorsal flank of recipient mice. The resulting tumors were harvested 2 to 7 days postinjection for analysis. B, proliferation of tumor cells in proximity to exogenous EC (blue*) within the interior of the tumors for WT versus KO EC was quantified on the basis of nuclear PCNA staining (arrowheads), 4 days posttransplantation ($P < 0.05$), and proliferation in the tumor periphery, where tumor cells are proximal to host blood vessels (arrows). Right, lower magnification photomicrographs, with boxed areas indicating regions shown in higher magnification on the left. Scale bar = 10 μm (left), 50 μm (right). C, tumor volume was scored over time at days 2, 4, and 7 posttransplantation. D, schematic for tumor cell–endothelial cell CM cotransplantation experimental design. 4T1 tumor cells were ad-mixed with 5× concentrated CM from WT or KO EC versus control base medium, resuspended in growth factor–reduced Matrigel, and injected subcutaneously into the dorsal flank of recipient mice. The resulting tumors were harvested 7 days postinjection for analysis. Tumor volume was measured at day 7. Data were consolidated from 6 to 10 independent animals/condition in at least 2 experiments, using CM/cells from at least 3 independent WT versus KO EC isolates for all *in vivo* studies. Graphs display average ± SD.

High levels of EphA2 are associated with low Slit2 expression in tumor endothelium, and Slit2 expression predicts good prognosis in human breast cancer

To evaluate clinical relevance, we assessed EphA2 and Slit2 protein in human breast cancer TMAs in which we could distinguish expression in tumor vessels from tumor epithelium and other stromal components. Slit2 protein was absent within a significant number of EphA2-positive tumor vessels in human invasive ductal breast carcinoma specimens (36 EphA2+/Slit2− samples out of 53), whereas significantly fewer EphA2-positive tumor vessels coexpressed Slit2 (17 EphA2+/Slit2+ samples out of 53; $P = 0.009$; Fig. 5A). We confirmed specificity of anti-EphA2 staining using mouse mammary tissue from WT versus KO MMTV-Neu tumors (Fig. 5B; ref. 29). In addition, we observed strong Slit2 protein expression in normal/hyperplastic human breast epithelium in TMAs, but not in tumor epithelium from stage II invasive breast cancer samples (Fig. 5B). Thus, these expression patterns suggest that EphA2 may also negatively regulate Slit2 in human breast tumor endothelium.

Slit2 has been reported to display tumor suppressor activity and/or to be inactivated in several types of cancer, including

Published OnlineFirst December 8, 2010; DOI:10.1158/0008-5472.CAN-10-3396

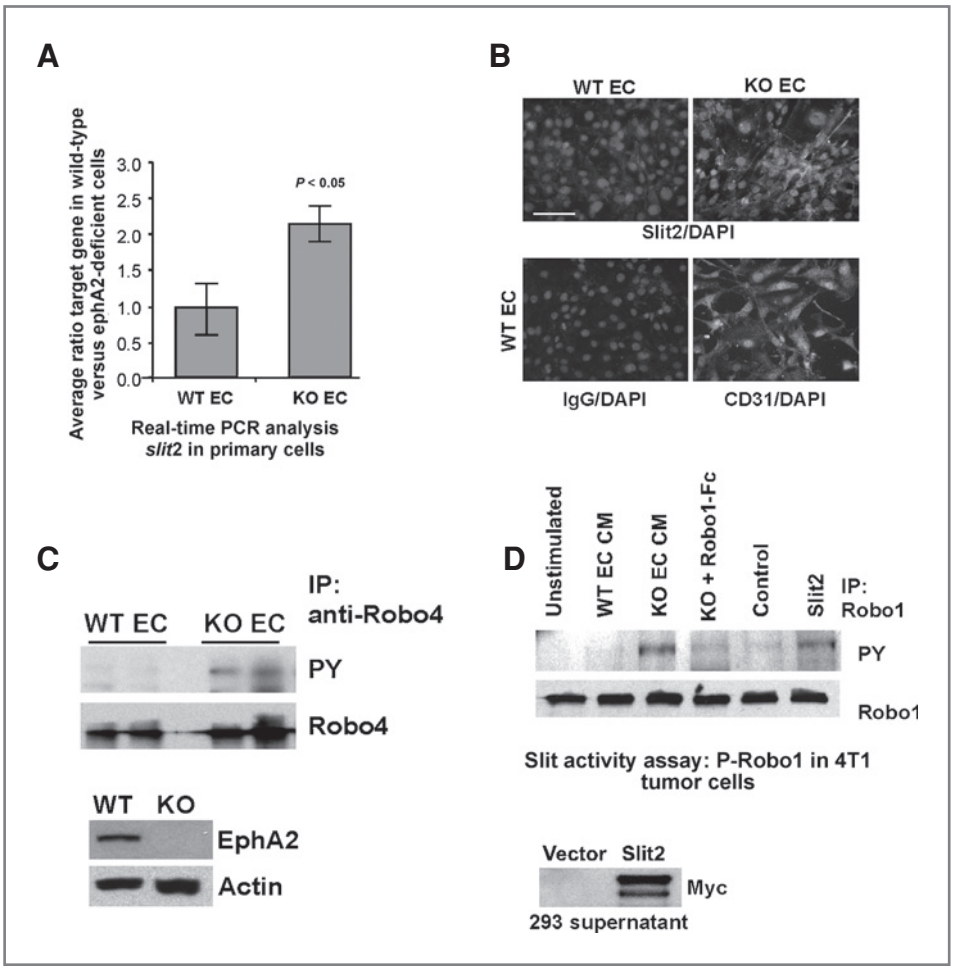

Figure 3. Slit2 expression and activity are elevated in EphA2-deficient endothelial cells. A, *slit2* expression in WT versus KO EC was measured by real-time qRT-PCR analysis. Expression was analyzed using RNA harvested from 5 independent EC isolates/genotype. Graph displays average ± SD. B, Slit2 protein was detected in EC by immunofluorescence staining. Staining for the endothelial cell marker CD31 was performed to confirm that greater than 95% of the cells in isolates were of endothelial origin. Scale bar = 20 μm. C, to correlate expression data with Slit function, phosphorylation of Robo4 receptor in WT versus KO EC was used as a surrogate for Slit activity. The absence of EphA2 protein expression in KO EC lysates versus WT EC was confirmed by immunoblot analysis. Blots were stripped and reprobed for actin to validate uniform loading. D, to determine whether Slit activity present in EC CM affected tumor cells, phosphorylation of Robo1 receptor in 4T1 tumor cells was assessed on stimulation with 10× CM from WT versus KO EC (±soluble Robo1-Fc) versus base medium (negative control) or recombinant Slit2 (positive control) after Robo1 immunoprecipitation. Expression of myc-tagged, recombinant Slit2 in HEK293 producer cell lysates was confirmed by immunoblot analysis.

breast (13, 16, 25, 37–48). On the other hand, independent studies provide evidence that Slit2 promotes tumor lymphatic metastasis in the RIP-tag transgenic mouse model of islet cell carcinoma (19), and motility and invasiveness of breast cancer cell lines that preferentially metastasize to brain (15). Given the controversial role of Slit2 in cancer, we investigated *slit2* expression in published human breast cancer microarray data sets from panels of 295, 117, and 286 breast cancer samples (33–35). High levels of *slit2* were associated with better overall (van de Vijver data set; ref. 33) and recurrence-free/metastsis-free (van de Vijver, van't Veer, and Wang data sets; refs. 33–35) survival on the basis of Kaplan–Meier analyses. (Fig. 5C; Supplementary Fig. S4A and B). Cox model analysis supported the observed associations between *slit2* and overall survival (van de Vijver data set; ref. 33; hazard ratio of *slit2* expression is 0.092, with 95% CI lower band of 0.02 and upper band of 0.4, $P = 0.0008$). These data support a tumor suppressive role for Slit2 in breast cancer, highlighting the clinical relevance of Slit2 and EphA2, and support the hypothesis that EphA2 downregulates Slit2 in endothelium to facilitate angiocrine-mediated tumor progression.

Discussion

Interaction between malignant cells and associated tumor vessels is crucial for tumor cell growth, survival, and metastatic spread (reviewed in refs. 1, 5). Apart from these functions, however, the role that endothelium plays in direct molecular regulation of tumor cell behavior remains understudied. Our laboratory and others have established Eph RTKs and ephrin ligands as key regulators of physiologic and pathologic angiogenesis, particularly in cancer (reviewed in refs. 9, 49). We now

Published OnlineFirst December 8, 2010; DOI:10.1158/0008-5472.CAN-10-3396

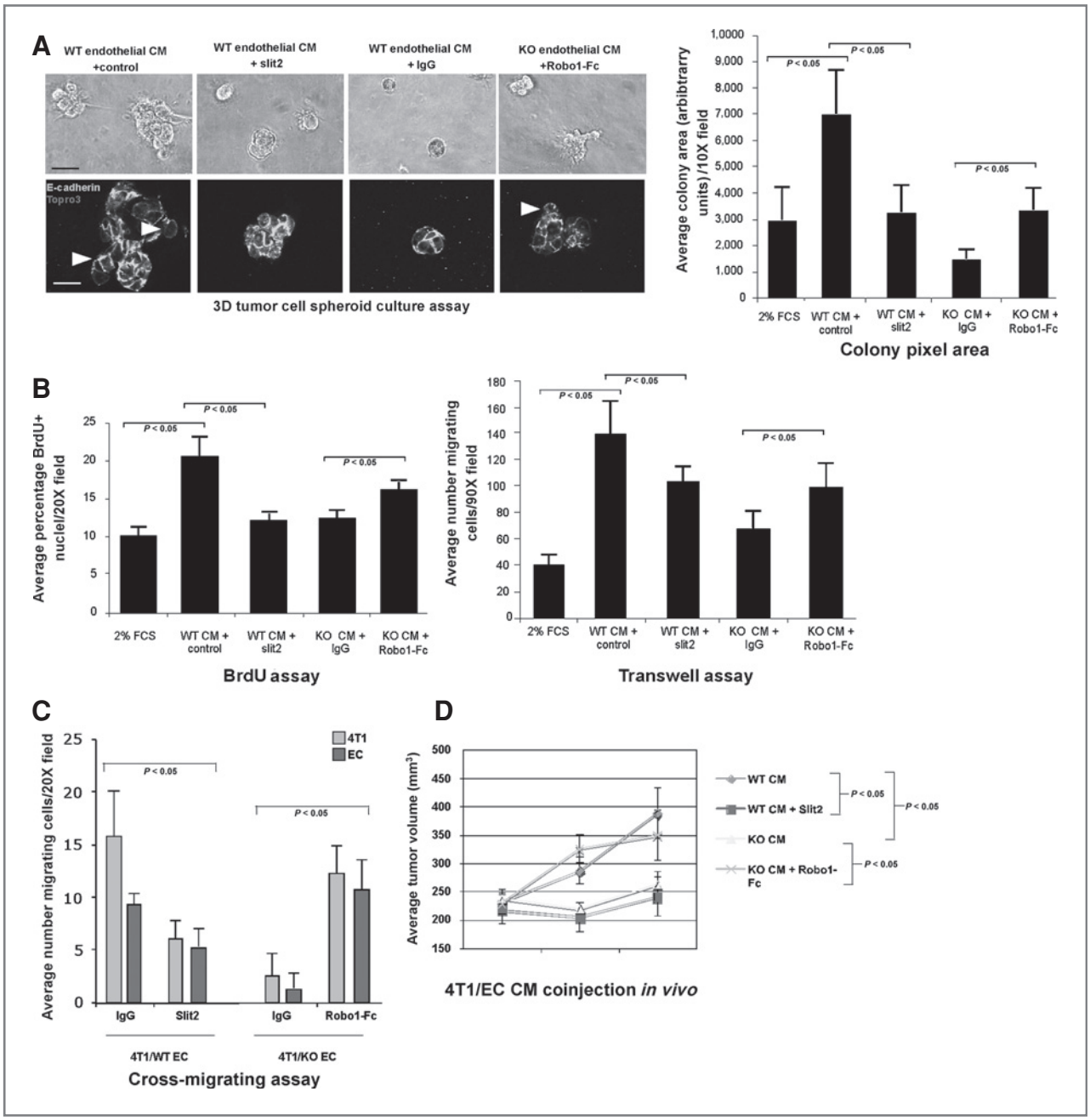

Figure 4. Modulating Slit2 activity in endothelium affects angiocrine-mediated tumor growth and motility in the context of endothelial EphA2 receptor function. A, top, photomicrographs of 4T1 tumor cell spheroids cultured in WT EC CM ± recombinant Slit2/control IgG or KO EC CM ± soluble Robo1-Fc/control IgG for 5 days. Bottom, confocal images of spheroids stained with E-cadherin and Topro3 nuclear counterstain. Arrowheads indicate invasive protrusions. Scale bar = 25 μm (top), 10 μm (bottom). Colony size was quantified on the basis of pixel area of 4 independent colonies/photomicrograph in replicate cultures from 3 to 5 independent experiments. Graph displays average ± SD. B, 4T1 tumor cell proliferation was quantified in 2D culture by BrdU incorporation, and 4T1 tumor cell migration was measured by transwell assay. C, cross-migration of tumor cells and endothelial cells was quantified simultaneously on the basis of cell morphology and differential fluorescent labeling in microfluidic chamber devices. Data are a representation of 3 to 5 independent experiments using CM from at least 3 independent WT versus KO EC isolates for all cell culture experiments. Graphs display average ± SD. D, 4T1 tumor cells were ad-mixed with 5× concentrated WT EC CM ± Slit2/control IgG or KO EC CM ± Robo1-Fc/control IgG, resuspended in growth factor–reduced Matrigel, and injected subcutaneously into the dorsal flank of recipient mice. Tumor dimensions were measured at 1, 3, and 7 days postinjection for comparison of tumor volume over time, and harvested on day 7 for analysis. Data were consolidated from 6 to 10 independent animals/condition in at least 2 experiments for *in vivo* studies. Graph displays average ± SD.

Published OnlineFirst December 8, 2010; DOI:10.1158/0008-5472.CAN-10-3396

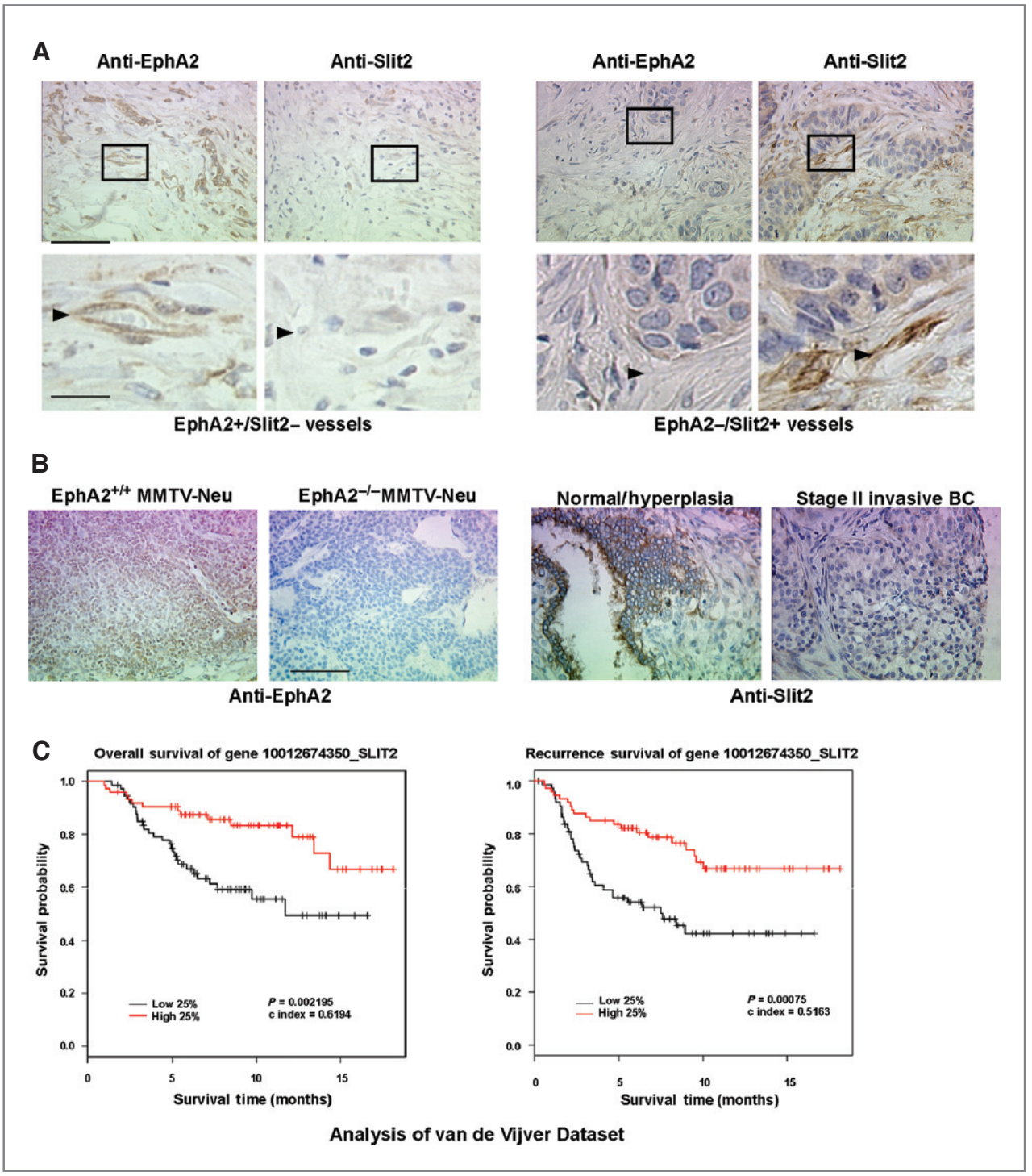

Figure 5. EphA2 and Slit2 expression profiles in human breast cancer. A, EphA2 and Slit2 protein expression in human invasive ductal carcinoma samples was analyzed in breast cancer TMA (Cybrdi, Inc.). Representative photographs of EphA2-negative /Slit2-positive tumor blood vessels (left), and of EphA2-positive/Slit2-negative (right) tumor blood vessels, are shown. Arrowheads indicate tumor blood vessels. Of the 53 samples, 17 harbored EphA2-positive/Slit2-positive tumor vessels, compared with 36 out of 53 samples with tumor vessels that were EphA2-postive/Slit2-negative ($P = 0.009$, χ^2 test). Scale bar = 50 μm (top), 10 μm (bottom). B, controls for EphA2 antibody specificity. MMTV-Neu tumor tissue sections from EphA2 WT and KO animals were stained with anti-EphA2 antibodies. Slit2 protein was detected in tumor parenchyma of normal/hyperplastic human breast tissue epithelium, but not in tumor epithelium from stage II invasive breast cancer, in TMA samples. Scale bar = 50 μm. C, Kaplan–Meier kinetic analyses of the van der Vijver data set, with microarray profiles of 295 human breast tumors and associated clinical data. The impact of elevated *slit2* expression on overall survival and recurrence-free survival was analyzed by log-rank tests.

Published OnlineFirst December 8, 2010; DOI:10.1158/0008-5472.CAN-10-3396

report that although WT EC produce soluble signals that enhance tumor cell proliferation and migration, these angiocrine-mediated effects are reduced in response to EphA2 KO EC. KO EC express elevated levels of *slit2* and secrete more active Slit protein. Moreover, inhibiting Slit activity in KO EC partially rescued tumor cell proliferation and motility, whereas Slit2 gain-of-function abrogated proliferation and motility induced by WT EC. Our data show that signals emanating from endothelium can influence tumor growth and migration, processes that are crucial for tumor progression, independent of their function in oxygen and nutrient transport.

Slit proteins, including the prototypical *Drosophila* Slit and vertebrate Slits 1–3, bind to roundabout receptors (Robo 1–4 in vertebrates) to regulate diverse cellular processes including axon repulsion, lymphocyte chemotaxis, and angiogenesis (reviewed in refs. 36, 50–52). Although the role of Slit proteins in tumor progression is somewhat controversial, several reports provide evidence that these molecules can function as tumor suppressors, particularly in breast cancer. Prasad and colleagues (14) reported that Robo1 and Robo2 receptors are expressed in human breast cancer samples, and that Slit2 negatively regulates chemokine-induced cancer cell chemotaxis, invasion, and adhesion, suggesting that Slit–Robo interaction may suppress metastatic spread in breast cancer. Slit2 overexpression in breast cancer cell lines inhibited colony formation in soft agar, and treatment with recombinant Slit2 suppressed tumor cell growth *in vitro* (13). More recent studies reported that Slit2 or Slit3 overexpressing breast cancer cells display reduced tumor growth *in vivo* (16, 45). Slit2/3-deficient mammary epithelium displays hyperplasia when transplanted into the cleared fat pad of recipient host mice (45). In addition, Slit2 was reported to inhibit breast cancer cell migration in response to hepatocyte growth factor (48), suggesting that Slit2 suppresses tumor cell motility and growth. Taken together, these data suggest that autocrine Slit2 can inhibit tumor growth and invasion in human cancer. Indeed, we found a strong and significant correlation between high levels of *slit2* expression and better overall and/or recurrence or metastasis-free survival in 3 large, independent human breast cancer patient data sets, and mutually exclusive expression of EphA2 and Slit2 within tumor endothelium in a significant portion of invasive human breast cancer patient samples. These data support a tumor suppressive role for Slit2 in human breast cancer, and the relevance of EphA2 mediated repression of Slit2 produced by tumor endothelium. We believe that there are other factors differentially expressed between WT versus KO EC that could be involved in suppression on the basis of our microarray analysis, and we are currently working to validate such candidate factors and elucidate their role in angiocrine signaling.

In summary, our data support the role of "angiocrine" signals in tumor growth and motility regulation. In addition, we show that endothelium not only upregulates progrowth and chemotaxis signals, but also reduces expression of tumor suppressive factors. EphA2 suppression of *slit2* in endothelium is a critical component of this mechanism, alleviating its antigrowth and chemorepulsive effects in breast tumor cells. Thus, endothelial cells could provide an initial growth advantage, and chemotactic cues, to tumor epithelium prior to and/or in addition to functional vessel formation. Given the antigrowth and chemorepulsive functions of Slit2, it is plausible that juxtacrine signaling between endothelial cell–expressed Slit2 and adjacent epithelial cells could suppress cellular growth and motility in normal tissue to maintain homeostasis. Activation of EphA2 receptor on endothelial cells by ephrin ligands expressed on adjacent endothelial cells or tumor cells could lead to Slit2 repression, thus creating a permissive environment for growth and invasion. This study, and other recent investigations into endothelial cell–tumor cell communication (53–56), validate the crucial role of angiocrine signaling on tumor growth and migration, which may provide new treatment options designed to sustain tumor dormancy and/or prevent recurrence and metastasis by targeting angiocrine regulators such as EphA2.

Disclosure of Potential Conflicts of Interest

No potential conflicts of interest were disclosed.

Acknowledgments

We thank Drs. Vivian Siegel, Lynn Matrisian, Mary Zutter, Pampee Young, and Rebecca Cook at Vanderbilt University for helpful comments and discussion.

Grant Support

This work was supported by the Department of Veterans Affairs through a VA Merit Award (J. Chen) and NIH grants CA95004 and CA114301 (J. Chen). D. M. Brantley-Sieders is supported by NIH grant CA1179151. M. Rao is supported by Department of Defense Breast Cancer Research Program Grant W81XWH-10-1-0256. Y. Shyr and A. Jiang are supported by the Vanderbilt-Ingram Cancer Center Biostatistics Shared Resource NCI Grant P30 CA68485. Y. Gao and D. Li are supported by NSF grant CBET0643583. S. Short is supported by NCI training grant T32 CA09592-21, 22 (L. Matrisian). J.Y. Wu is supported by NIH grants CA114197 and CA107193, and by the James S. McDonnell Foundation.

The costs of publication of this article were defrayed in part by the payment of page charges. This article must therefore be hereby marked *advertisement* in accordance with 18 U.S.C. Section 1734 solely to indicate this fact.

Received October 15, 2010; revised November 1, 2010; accepted November 11, 2010; published OnlineFirst December 8, 2010.

References

1. Chung AS, Lee J, Ferrara N. Targeting the tumour vasculature: insights from physiological angiogenesis. Nat Rev Cancer 10;505–14.
2. Folkman J. What is the evidence that tumors are angiogenesis dependent?J Natl Cancer Inst 1990;82:4–6.
3. Weidner N, Cady B, Goodson WH 3rd. Pathologic prognostic factors for patients with breast carcinoma. Which factors are important. Surg Oncol Clin N Am 1997;6:415–62.
4. Gasparini G. Clinical significance of determination of surrogate markers of angiogenesis in breast cancer. Crit Rev Oncol Hematol 2001;37:97–114.
5. Bergers G, Benjamin LE. Tumorigenesis and the angiogenic switch. Nat Rev Cancer 2003;3:401–10.
6. Cao Y. Molecular mechanisms and therapeutic development of angiogenesis inhibitors. Adv Cancer Res 2008;100:113–31.

Published OnlineFirst December 8, 2010; DOI:10.1158/0008-5472.CAN-10-3396

7. Shojaei F, Ferrara N. Role of the microenvironment in tumor growth and in refractoriness/resistance to anti-angiogenic therapies. Drug Resist Updat 2008;11:219–30.
8. Butler JM, Kobayashi H, Rafii S. Instructive role of the vascular niche in promoting tumour growth and tissue repair by angiocrine factors. Nat Rev Cancer 10;138–46.
9. Brantley-Sieders DM, Chen J. Eph receptor tyrosine kinases in angiogenesis: from development to disease. Angiogenesis 2004; 7:17–28.
10. Ahmed Z, Bicknell R. Angiogenic signalling pathways. Methods Mol Biol 2009;467:3–24.
11. Pasquale EB. Eph receptors and ephrins in cancer: bidirectional signalling and beyond. Nat Rev Cancer 10;165–80.
12. Killeen MT, Sybingco SS. Netrin, Slit and Wnt receptors allow axons to choose the axis of migration. Dev Biol 2008;323:143–51.
13. Dallol A, Da Silva NF, Viacava P, Minna JD, Bieche I, Maher ER, et al. SLIT2, a human homologue of the Drosophila Slit2 gene, has tumor suppressor activity and is frequently inactivated in lung and breast cancers. Cancer Res 2002;62:5874–80.
14. Prasad A, Fernandis AZ, Rao Y, Ganju RK. Slit protein-mediated inhibition of CXCR4-induced chemotactic and chemoinvasive signaling pathways in breast cancer cells. J Biol Chem 2004;279: 9115–24.
15. Schmid BC, Rezniczek GA, Fabjani G, Yoneda T, Leodolter S, Zeillinger R. The neuronal guidance cue Slit2 induces targeted migration and may play a role in brain metastasis of breast cancer cells. Breast Cancer Res Treat 2007;106:333–42.
16. Prasad A, Paruchuri V, Preet A, Latif F, Ganju RK. Slit-2 induces a tumor-suppressive effect by regulating beta-catenin in breast cancer cells. J Biol Chem 2008;283:26624–33.
17. Wang LJ, Zhao Y, Han B, Ma YG, Zhang J, Yang DM, et al. Targeting Slit-Roundabout signaling inhibits tumor angiogenesis in chemical-induced squamous cell carcinogenesis. Cancer Sci 2008;99: 510–7.
18. Yiin JJ, Hu B, Jarzynka MJ, Feng H, Liu KW, Wu JY, et al. Slit2 inhibits glioma cell invasion in the brain by suppression of Cdc42 activity. Neuro Oncol 2009; 11:779–89.
19. Yang XM, Han HX, Sui F, Dai YM, Chen M, Geng JG. Slit-Robo signaling mediates lymphangiogenesis and promotes tumor lymphatic metastasis. Biochem Biophys Res Commun 396:571–7.
20. Brantley-Sieders DM, Caughron J, Hicks D, Pozzi A, Ruiz JC, Chen J. EphA2 receptor tyrosine kinase regulates endothelial cell migration and vascular assembly through phosphoinositide 3-kinase-mediated Rac1 GTPase activation. J Cell Sci 2004;117:2037–49.
21. Langley RR, Ramirez KM, Tsan RZ, Van Arsdall M, Nilsson MB, Fidler IJ. Tissue-specific microvascular endothelial cell lines from H-2K(b)-tsA58 mice for studies of angiogenesis and metastasis. Cancer Res 2003;63:2971–6.
22. Fang WB, Brantley-Sieders DM, Hwang Y, Ham AJ, Chen J. Identification and functional analysis of phosphorylated tyrosine residues within EphA2 receptor tyrosine kinase. J Biol Chem 2008;283:16017–26.
23. Muraoka RS, Koh Y, Roebuck LR, Sanders ME, Brantley-Sieders D, Gorska AE, et al. Increased malignancy of Neu-induced mammary tumors overexpressing active transforming growth factor beta1. Mol Cell Biol 2003;23:8691–703.
24. Wu JY, Feng L, Park HT, Havlioglu N, Wen L, Tang H, et al. The neuronal repellent Slit inhibits leukocyte chemotaxis induced by chemotactic factors. Nature 2001;410:948–52.
25. Mertsch S, Schmitz N, Jeibmann A, Geng JG, Paulus W, Senner V. Slit2 involvement in glioma cell migration is mediated by Robo1 receptor. J Neurooncol 2008;87:1–7.
26. Jones CA, London NR, Chen H, Park KW, Sauvaget D, Stockton RA, et al. Robo4 stabilizes the vascular network by inhibiting pathologic angiogenesis and endothelial hyperpermeability. Nat Med 2008; 14:448–53.
27. Yuasa-Kawada J, Kinoshita-Kawada M, Rao Y, Wu JY. Deubiquitinating enzyme USP33/VDU1 is required for Slit signaling in inhibiting breast cancer cell migration. Proc Natl Acad Sci U S A 2009;106: 14530–5.
28. Debnath J, Muthuswamy SK, Brugge JS. Morphogenesis and oncogenesis of MCF-10A mammary epithelial acini grown in three-dimensional basement membrane cultures. Methods 2003;30:256–68.
29. Brantley-Sieders DM, Zhuang G, Hicks D, Fang WB, Hwang Y, Cates JM, et al. The receptor tyrosine kinase EphA2 promotes mammary adenocarcinoma tumorigenesis and metastatic progression in mice by amplifying ErbB2 signaling. J Clin Invest 2008;118: 64–78.
30. Brantley-Sieders DM, Fang WB, Hicks DJ, Zhuang G, Shyr Y, Chen J. Impaired tumor microenvironment in EphA2-deficient mice inhibits tumor angiogenesis and metastatic progression. FASEB J 2005; 19:1884–6.
31. Brantley DM, Cheng N, Thompson EJ, Lin Q, Brekken RA, Thorpe PE, et al. Soluble Eph A receptors inhibit tumor angiogenesis and progression in vivo. Oncogene 2002;21:7011–26.
32. Brantley-Sieders DM, Fang WB, Hwang Y, Hicks D, Chen J. Ephrin-A1 facilitates mammary tumor metastasis through an angiogenesis-dependent mechanism mediated by EphA receptor and vascular endothelial growth factor in mice. Cancer Res 2006;66: 10315–24.
33. van de Vijver MJ, He YD, van't Veer LJ, Dai H, Hart AA, Voskuil DW, et al. A gene-expression signature as a predictor of survival in breast cancer. N Engl J Med 2002;347:1999–2009.
34. van't Veer LJ, Dai H, van de Vijver MJ, He YD, Hart AA, Mao M, et al. Gene expression profiling predicts clinical outcome of breast cancer. Nature 2002;415:530–6.
35. Wang Y, Klijn JG, Zhang Y, Sieuwerts AM, Look MP, Yang F, et al. Gene-expression profiles to predict distant metastasis of lymph-node-negative primary breast cancer. Lancet 2005;365:671–9.
36. Legg JA, Herbert JM, Clissold P, Bicknell R. Slits and Roundabouts in cancer, tumour angiogenesis and endothelial cell migration. Angiogenesis 2008;11:13–21.
37. Dallol A, Krex D, Hesson L, Eng C, Maher ER, Latif F. Frequent epigenetic inactivation of the SLIT2 gene in gliomas. Oncogene 2003;22:4611–6.
38. Astuti D, Da Silva NF, Dallol A, Gentle D, Martinsson T, Kogner P, et al. SLIT2 promoter methylation analysis in neuroblastoma, Wilms' tumour and renal cell carcinoma. Br J Cancer 2004;90:515–21.
39. Dammann R, Strunnikova M, Schagdarsurengin U, Rastetter M, Papritz M, Hattenhorst UE, et al. CpG island methylation and expression of tumour-associated genes in lung carcinoma. Eur J Cancer 2005;41:1223–36.
40. Narayan G, Goparaju C, Arias-Pulido H, Kaufmann AM, Schneider A, Durst M, et al. Promoter hypermethylation-mediated inactivation of multiple Slit-Robo pathway genes in cervical cancer progression. Mol Cancer 2006;5:16.
41. Werbowetski-Ogilvie TE, Seyed Sadr M, Jabado N, Angers-Loustau A, Agar NY, Wu J, et al. Inhibition of medulloblastoma cell invasion by Slit. Oncogene 2006;25:5103–12.
42. Sharma G, Mirza S, Prasad CP, Srivastava A, Gupta SD, Ralhan R. Promoter hypermethylation of p16INK4A, p14ARF, CyclinD2 and Slit2 in serum and tumor DNA from breast cancer patients. Life Sci 2007;80:1873–81.
43. Singh RK, Indra D, Mitra S, Mondal RK, Basu PS, Roy A, et al. Deletions in chromosome 4 differentially associated with the development of cervical cancer: evidence of slit2 as a candidate tumor suppressor gene. Hum Genet 2007;122:71–81.
44. Kim HK, Zhang H, Li H, Wu TT, Swisher S, He D, et al. Slit2 inhibits growth and metastasis of fibrosarcoma and squamous cell carcinoma. Neoplasia 2008;10:1411–20.
45. Marlow R, Strickland P, Lee JS, Wu X, Pebenito M, Binnewies M, et al. SLITs suppress tumor growth in vivo by silencing Sdf1/Cxcr4 within breast epithelium. Cancer Res 2008;68:7819–27.
46. Dietrich D, Lesche R, Tetzner R, Krispin M, Dietrich J, Haedicke W, et al. Analysis of DNA methylation of multiple genes in microdissected cells from formalin-fixed and paraffin-embedded tissues. J Histochem Cytochem 2009;57:477–89.
47. Dunwell TL, Dickinson RE, Stankovic T, Dallol A, Weston V, Austen B, et al. Frequent epigenetic inactivation of the SLIT2 gene in chronic and acute lymphocytic leukemia. Epigenetics 2009;4:265–9.

Published OnlineFirst December 8, 2010; DOI:10.1158/0008-5472.CAN-10-3396

48. Stella MC, Trusolino L, Comoglio PM. The Slit/Robo system suppresses hepatocyte growth factor-dependent invasion and morphogenesis. Mol Biol Cell 2009;20:642–57.
49. Kuijper S, Turner CJ, Adams RH. Regulation of angiogenesis by Eph-ephrin interactions. Trends Cardiovasc Med 2007;17:145–51.
50. Fernandis AZ, Ganju RK. Slit: a roadblock for chemotaxis. Sci STKE 2001;2001:PE1.
51. Dickson BJ, Gilestro GF. Regulation of commissural axon pathfinding by slit and its Robo receptors. Annu Rev Cell Dev Biol 2006;22:651–75.
52. Hohenester E. Structural insight into Slit-Robo signalling. Biochem Soc Trans 2008;36:251–6.
53. Hatfield K, Ryningen A, Corbascio M, Bruserud O. Microvascular endothelial cells increase proliferation and inhibit apoptosis of native human acute myelogenous leukemia blasts. Int J Cancer 2006;119:2313–21.
54. De Bruyne E, Andersen TL, De Raeve H, Van Valckenborgh E, Caers J, Van Camp B, et al. Endothelial cell-driven regulation of CD9 or motility-related protein-1 expression in multiple myeloma cells within the murine 5T33MM model and myeloma patients. Leukemia 2006;20:1870–9.
55. Barrett JM, Mangold KA, Jilling T, Kaul KL. Bi-directional interactions of prostate cancer cells and bone marrow endothelial cells in three-dimensional culture. Prostate 2005;64:75–82.
56. Barrett JM, Rovedo MA, Tajuddin AM, Jilling T, Macoska JA, MacDonald J, et al. Prostate cancer cells regulate growth and differentiation of bone marrow endothelial cells through TGFbeta and its receptor, TGFbetaRII. Prostate 2006;66:632–50.